Supporting Information

Wang et al. 10.1073/pnas.1013101108

SI Methods

Protein Preparation. The DNA fragments encoding Ent3p_ENTH domain (uniprotKB ID: P47160; amino residues 28–170) and Vti1p_Habc domain (uniprotKB ID: Q04338; amino residues 3–99) were amplified by polymerase chain reaction (PCR) from *Saccharomyces cerevisiae* genome and subcloned into the modified pET22b+. They were then transformed into the *Escherichia coli* expression strain Rossetta (DE3). Both proteins were overexpressed in the cells with His-tag (MGHHHHHHMENLYFQSLMSVDP- for yENTH, and MGHHHHHHMENLYFQ- for yHabc) fused to their N terminus and induced by IPTG at 289 K in LB medium. Affinity chromatography with a Chelating Sepharose™ Fast Flow (Amersham Biosciences) was used as the first step of the purification. Purified proteins were then incubated with His-tagged TEV protease at 289 K to cleave the His-tag. After the overnight cleavage, samples were changed to 20 mM Tris-HCl pH 7.5, 400 mM NaCl, and 40 mM imidazole and passed through a Chelating affinity chromatography column to remove TEV protease and the cleaved His-tag. Size exclusion chromatography on a Superdex 75 column (16 × 120 mm, Amersham Biosciences) was performed to final purification. yENTH–yHabc complex was isolated by a size exclusion chromatography on a Superdex 75 column after mixing together these two proteins. All proteins (yENTH, yHabc, and their complex) were concentrated to 10 mg/mL in 20 mM Tris-HCl, and 200 mM NaCl before crystallization.

Crystallization. Crystallization of the proteins was performed at 288 K using a hanging-drop vapor diffusion method. Each drop was mixed by 2 μL protein and 2 μL reservoir solution to equilibrate against 200 μL reservoir solution. yHabc was crystallized in 0.2 M Ammonium Sulfate, 0.1 M Sodium Acetate pH 4.6 and 25% w/v PEG4000; yENTH was crystallized in 8% tacsimate pH 4.0 and 20% w/v PEG3350; yENTH-yHabc complex was crystallized in 0.2 M tri-Lithium Citrate and 20% w/v PEG3350.

Data Collection, Phase Determination, and Structure Refinement. The yHabc crystals were soaked in a cryoprotectant solution (0.16 M Ammonium Sulfate, 0.08 M Sodium Acetate pH 4.6, 20% w/v PEG4000, and 20% v/v glycerol) prior to data collection. The yENTH–yHabc complex crystals were passed through paraffin oil as cryoprotectant. X-ray diffraction data of yHabc crystal and the yENTH–yHabc complex crystal were collected on beamline 17U1 at Shanghai Synchrotron Radiation Facility. The yENTH crystals were soaked in a cryoprotectant solution (6% tacsimate pH 4.0, 16% w/v PEG3350, and 20% v/v glycerol). Diffraction data of the yENTH crystal were collected using a rotating-anode X-ray source (Cu Kα; RigakuMicro007) and an imaging plate (MAR Research dtb345), with a crystal-to-detector distance of 150 mm. All diffraction data were processed and scaled with the HKL2000 program (1). Structures of mouse vti1a_Habc (PDB ID code 1VCS) and human epsinR_ENTH (PDB ID code 1XGW) were used as the search models for molecular replacement in Molrep (2). Iterative model building and refinement were performed by using Coot (3), CNS (4), and Refmac5 (5). The quality of the final models was checked by Procheck (6). All current models have good geometry and no residues are in disallowed regions of the Ramachandran plot. Data collection and refinement statistics are listed in Table S1.

Sucrose Density Gradient Centrifugation and Size Exclusion Chromatography. Subcellular fractionation of osmotically lysed spheroplasts was performed as described on a density gradient with steps of 22%–55% sucrose (7). Cell homogenates cleared at 500 g_{max} were centrifuged for 16 hours at 135,000 g_{max}. Fractions were separated by SDS/PAGE and immunoblotted for Vti1p. Relative intensities of Vti1p in fractions obtained from one representative blot were plotted against fraction numbers. Size exclusion chromatography was performed as described (8) with these modifications: 100 OD of cells grown to an $OD_{600} = 1.0$ in YEPD were harvested, converted to spheroplasts and lysed by agitation with glass beads in 250 μL of buffer A (100 mM MES-NaOH, pH 6.5, 0.5 mM $MgCl_2$, 1 mM EGTA, 0.2 mM dithiothreitol and 10 mM NaN_3) with protease inhibitors. The lysate was centrifuged at 17,000 g_{max} for 30 min and the supernatant an additional 15 min at 17,000 g_{max}. The supernatant was loaded onto a 1.5 × 100 cm Sephacryl S-1000 column (GE Healthcare) coated with phosphatidylcholine liposomes. Fractions of 3 mL were collected. 1 mL of every other fraction was precipitated with 10% trichloroacetic acid in the presence of 25 μg bovine serum albumin, separated by SDS/PAGE and immunoblotted for Vti1p and Chc1p (9). Each strain was analyzed twice with comparable results with exception of variable clathrin signals in fraction 48.

Isothermal Titration Calorimetry (ITC). ITC experiments were performed on a MicroCal VP ITC unit at 298 K (MicroCal) in 20 mM Tris-HCl pH 7.5 and 200 mM NaCl. 0.73 mM yHabc was injected in 30 injections of 8 μl each to yENTH protein in the ITC cell (0.056 mM, 1.4 mL). Background heat of the dilution of yHabc protein into buffer alone was subtracted and titration curve was fitted by program ORIGIN, to give the stoichiometry n, equilibrium association constant $K_a(K_d^{-1})$ and enthalpy of binding.

Yeast Two-Hybrid and in Vitro Binding Assays. The yeast two-hybrid assay was performed as described (10) in L40 cells using pLexN with the N-terminal yHabc domain of Vti1p (amino acid residues 1–115), and pVP16-3 with the yENTH domain of Ent3p (amino acid residues 1–172) as well as the respective point mutants. Point mutations were introduced into Vti1p and Ent3p using PCRs with overlapping mutant oligonucleotides containing the mutation and a second PCR connecting both fragments. Yeast cells containing pairs of LexA DNA-binding domain and VP16 activation-domain fusions were streaked out on agar plates lacking tryptophan, histidine, uracil, leucine, and lysine (THULL). Expression of fusion proteins was checked by Western blotting. In vitro binding assays were done as described (11). Purified fusion proteins consisting of 6His-tagged Habc domain of Tlg1p (amino acid residues 1–137) or Vti1p (amino acid residues 1–115, 1.5 μM) and Strep-tagged yENTH domain of Ent3p (amino acid residues 1–172, 1 μM) were incubated in 100 μL PBS + 1% Triton X-100 + 10 mM imidazole for 30 min. 10 μL slurry of Ni-NTA beads were added and the incubation continued for another 30 min. Washed pellets were analyzed for Ent3p by immunoblotting.

Strains Used for in Vivo Experiments. The point mutations E17R, E42R or D46R were introduced into a 1.8 kb DNA fragment with the *VTI1* promoter and coding sequence in the centromeric vector pRS316. The point mutations E157R was introduced into a 1.8 kb DNA with the *ENT3* promoter and coding sequence in pRS316. The following strains were used for in vivo experiments: *ent5*Δ cells (BY4742 background) expressing Vti1p_D46R, *vti1*Δ *ent5*Δ cells (SEY6211 background, MGY2) expressing HA-Vti1p and Vti1p_E42R, *vti1*Δ cells (SEY6211 background, FvMY6)

(12) expressing Vti1p, Vti1p_E17R, Vti1p_E42R or Vti1p_D46R from centromeric vectors or *ent3*Δ cells (SEY6211 background, SCY13) (7) in the absence or presence of a plasmid encoding Ent3p_R157E.

1. Otwinowski Z, Minor W. (1997) Processing of X-ray diffraction data collected in oscillation mode. *Methods Enzymol* 276:307–326.
2. Vagin A, Teplyakov A (1997) Molrep: An automated program for molecular replacement. *J Appl Crystallogr* 30:1022–1025.
3. Emsley P, Cowtan K (2004) Coot: Model-building tools for molecular graphics. *Acta Crystallogr D Biol Crystallogr* 60:2126–2132.
4. Brunger AT, et al. (1998) Crystallography & NMR system: A new software suite for macromolecular structure determination. *Acta Crystallogr D Biol Crystallogr* 54:905–921.
5. Murshudov G, Vagin A, Dodson E (1997) Refinement of macromolecular structures by the maximum-likelihood method. *Acta Crystallogr D Biol Crystallogr* 53:240–255.
6. Laskowski RA, MacArthur MW, Moss DS, Thornton JM (1993) PROCHECK: A program to check the stereochemical quality of protein structures. *J Appl Crystallogr* 26:283–291.
7. Chidambaram S, Zimmermann J, von Mollard GF (2008) ENTH domain proteins are cargo adaptors for multiple SNARE proteins at the TGN endosome. *J Cell Sci* 121:329–338.
8. Fernandez GE, Payne GS (2006) Laa1p, a conserved AP-1 accessory protein important for AP-1 localization in yeast. *Mol Biol Cell* 17:3304–3317.
9. Lemmon S, Lemmon VP, Jones EW (1988) Characterization of yeast clathrin and anticlathrin heavy-chain monoclonal antibodies. *J Cell Biochem* 36:329–340.
10. Vojtek A, Hollenberg S (1995) Ras-Raf interaction: Two-hybrid analysis. *Methods Enzymol* 255:331–342.
11. Chidambaram S, Mullers N, Wiederhold K, Haucke V, von Mollard GF (2004) Specific interaction between SNAREs and epsin N-terminal homology (ENTH) domains of epsin-related proteins in trans-Golgi network to endosome transport. *J Biol Chem* 279:4175–4179.
12. von Mollard GF, Nothwehr SF, Stevens TH (1997) The yeast v-SNARE Vti1p mediates two vesicle transport pathways through interactions with the *t*-SNAREs Sed5p and Pep12p. *J Cell Biol* 137:1511–1524.

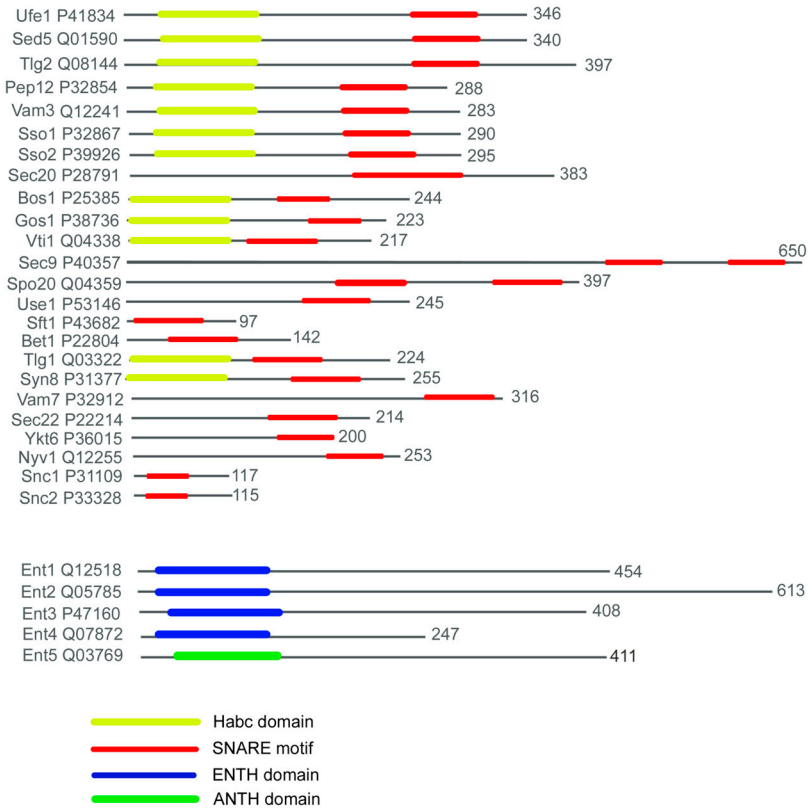

Fig. S1. List of 24 SNAREs and 5 Ent proteins in *Saccharomyces cerevisiae*. A total of 24 SNARE proteins are present in yeast, and more than 40 SNAREs are present in mammals. They vary greatly in size, combination with other domains, and are localized to different subcellular membranes. In contrast, the number of E/ANTH family members is limited, with only five Ent proteins in yeast and four in humans. Only a few Ent proteins are known to function as SNARE adaptor.

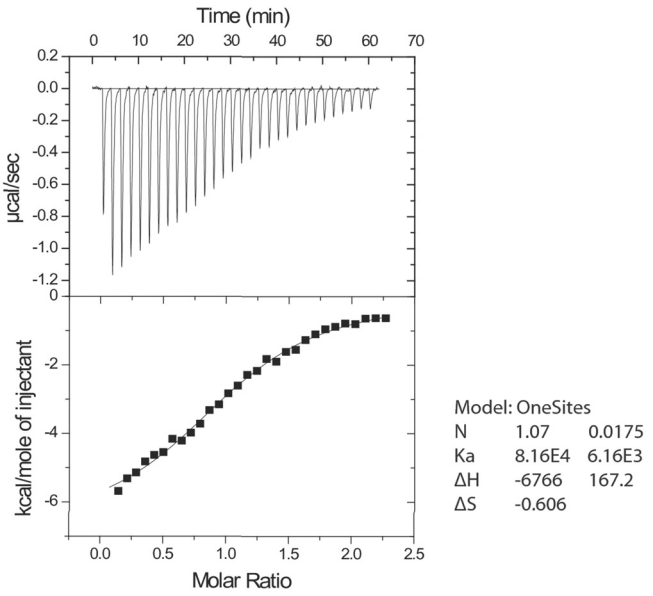

Fig. S2. ITC (isothermal titration calorimetry) assay of yeast Vti1p_Habc binding to yeast Ent3_ENTH. Yeast Vti1p_Habc interacts with Ent3_ENTH domain with a dissociation affinity of 12 µM and an interacting ratio of 1:1.

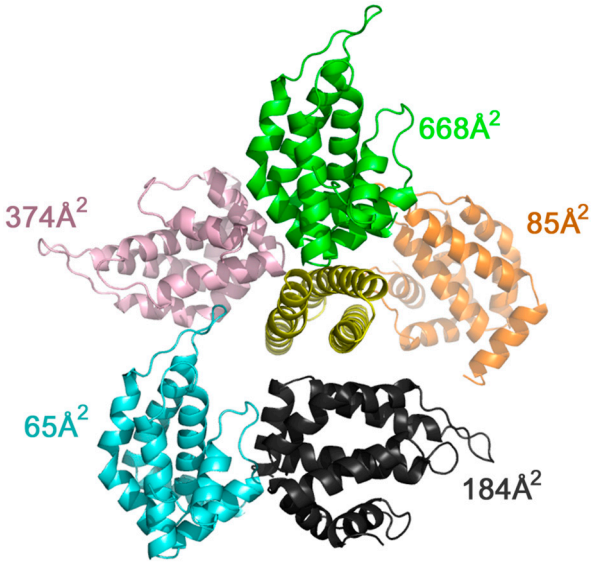

Fig. S3. Crystal packing of yeast Vti1p_Habc/Ent3_ENTH complex. The complex of yeast Vti1p_Habc (central, yellow)/Ent3_ENTH (green), which is verified in this work, represents the largest interface in the crystal packing. None of these packings is similar to the mammalian vti1b_Habc/epsinR_ENTH complex.

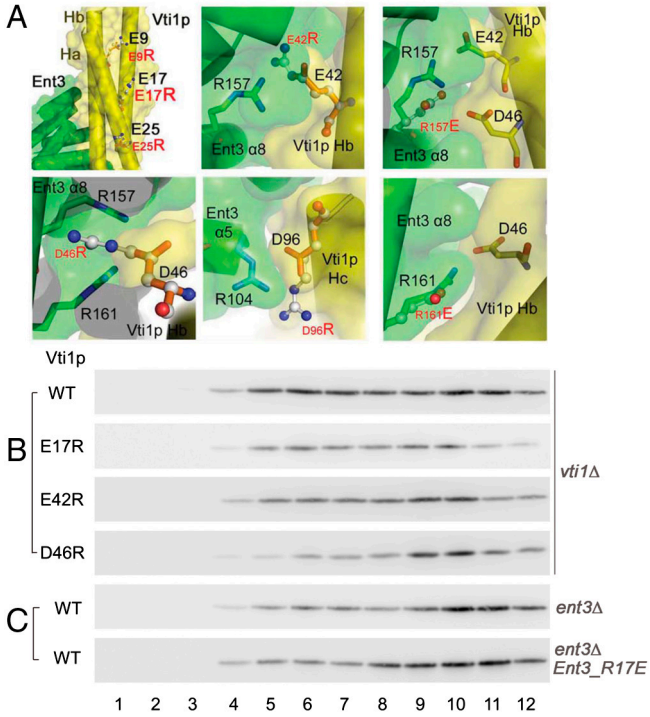

Fig. S4. Disruption of the Vti1p–Ent3p interaction changed the subcellular localization of Vti1p in yeast. (*A*) Detailed interfaces of yENTH–yHabc show the residues that were mutated in this work (yEnt3p_ENTH in green, yVti1p_Habc in yellow). Mutated side chains are also modeled and shown in white. (*B*) Homogenates of *vti1*Δ cells expressing Vti1p wt or mutants from centromeric vectors were analyzed by sucrose density gradient centrifugation and western blotting for Vti1p. Vti1p_E17R, which still binds to Ent3p, was similarly distributed as Vti1p_wt. In contrast, interface-disrupting mutants Vti1p_D46R was more abundant and Vti1p_E42R slightly more abundant in the denser fractions 10–12 than Vti1p_wt. These sorting defects of D46R and E42R were reproducible ($n = 3$). (*C*) Homogenates of *ent3*Δ cells (SCY13) expressing Vti1p in the absence or presence of a plasmid encoding Ent3p_R157E were analyzed as above. Distribution of Vti1p in *ent3*Δ was similar to the distribution of Vti1p_D46R in *vti1*Δ cells. Consistently, this distribution change could not be rescued by expressing an interaction-disrupting Ent3p mutant (Ent3p_R157E).

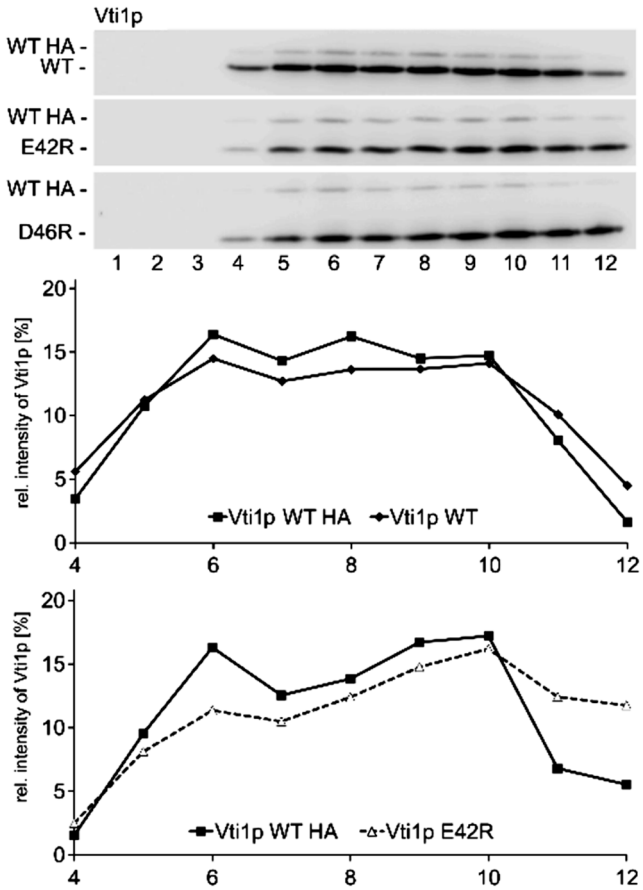

Fig. S5. Vti1p_E42R was slightly more abundant in denser fractions 11 and 12 than wild-type Vti1p. Cleared yeast homogenates from *vti1*Δ *ent5*Δ cells transformed with a HA-tagged Vti1p and a Vti1p, Vti1p_E42R, or Vti1p_D46R plasmid were fractionated on sucrose density gradients. Fractions were analyzed by immunoblotting for Vti1p. The relative intensities of Vti1p in the gradient fractions were plotted against the fraction number. Though small, the shifts in distribution of the mutant proteins were reproducible ($n = 3$). As control, fractionation of HA-Vti1p and Vti1p was compared and found to be similar. Fractionation behavior of Vti1p_D46R was similar in *ent5*Δ cells of BY4742 and SEY6211 background.

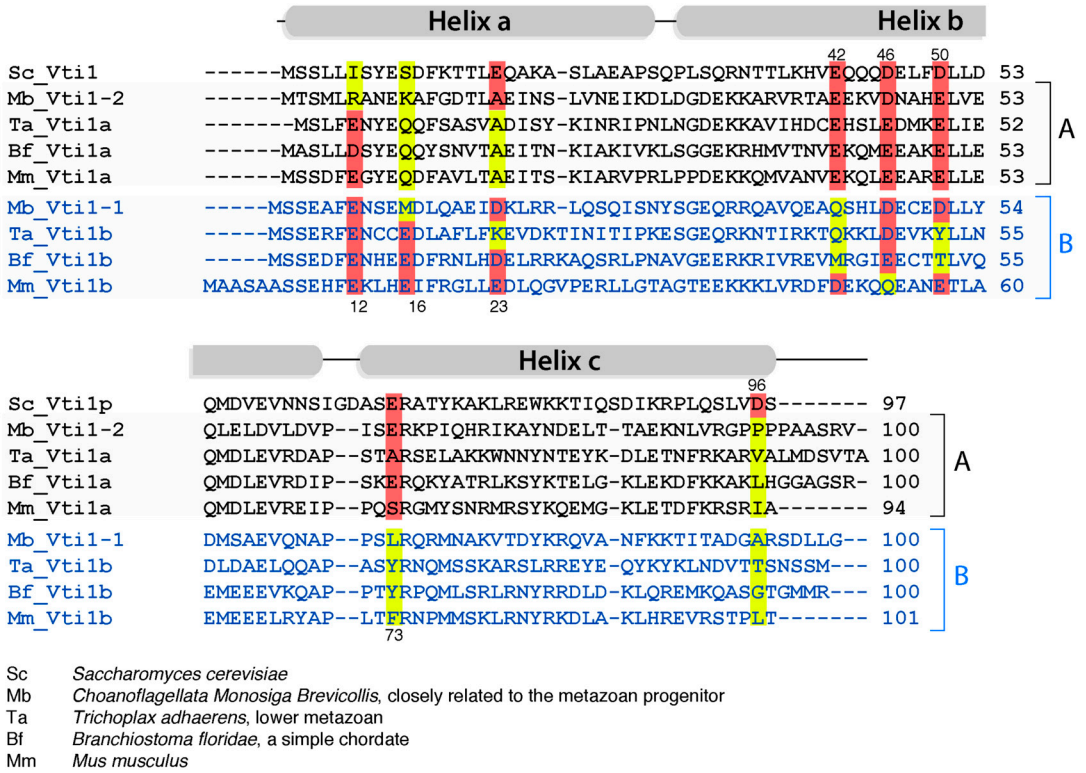

Fig. S6. Divergent sequences of Vti1_Habc suggest different sites to bind to ENTH domain. Vti1 proteins evolved from a single Vti1p in yeast to 2 subgroups in higher eukaryotes. The acidic patch on helix b (E42, E46, D50) is critical for yeast Vti1p to bind to yEnt3p_ENTH (Fig. 4). This acidic patch is conserved in yeast yVti1p and the higher eukaryotic Vti1a subgroup but not in Vti1b subgroup. Interestingly, another acidic patch on a different helix (helix a, E12, E16, E23) started to form later in the Vti1b subgroup. This acidic patch is found to bind epsinR_ENTH in mammals. Both acidic patches in yeast and mammalian Habc domains bind to the same region (α8) on ENTH domains. The divergence of the binding-site on Habc domains suggests there is a binding-site invention from yeast Vti1p to mammalian Vti1b during evolution.

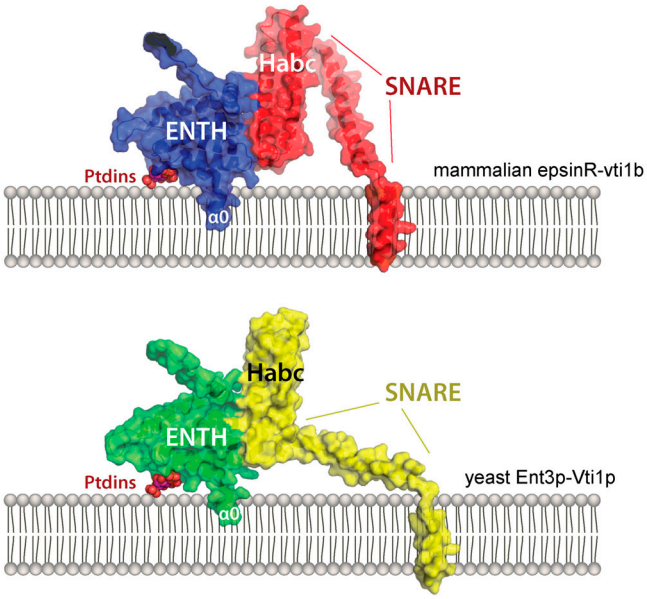

Fig. S7. Different membrane localization of SNARE motifs in yeast and mammal. The Vti1/ENTH complexes were modeled on to membrane by docking the additional N-terminal hydrophobic α0 helix of ENTH domain into the membrane. Because the orientations of Habc domains are opposite, yeast Ent3p and mammalian epsinR will have different membrane localization for their subsequent SNARE motifs.

Table S1. Data collection and refinement statistics

	yEnt3p_ENTH	yVti1p_Habc	yENTH-yHabc complex
Data collection			
Space group	*P*1	$P2_12_12_1$	$P2_12_12_1$
Cell dimensions			
a, b, c [Å]	$a = 26.600$, $b = 37.589$, $c = 38.109$	$a = 32.112$, $b = 49.751$, $c = 51.690$	$a = 58.683$, $b = 82.351$, $c = 95.953$
α, β, γ [°]	$\alpha = 77.81$, $\beta = 86.64$, $\gamma = 65.54$	$\alpha = \beta = \gamma = 90.00$	$\alpha = \beta = \gamma = 90.00$
Wavelength [Å]	1.5418	1.0000	1.0000
Resolution [Å]	40-2.1(2.18-2.10)*	50-1.92(1.95-1.92)	50-2.20(2.28-2.20)
R_{sym} or R_{merge} †	7.6(39.2)	9.1(30.5)	10.3(29.5)
$I/\sigma I$	12.2(2.3)	22.1(6.1)	12.2(5.9)
Completeness [%]	95.1(93.0)	99.4(94.7)	98.4(98.6)
Redundancy	2.1(2.1)	6.5(5.8)	6.1(5.0)
Refinement			
Resolution [Å]	37-2.09(2.14-2.09)	36-1.92(1.97-1.92)	43-2.20(2.26-2.20)
No. reflections	6612	6015	22512
R_{work}/R_{free} ‡,§	19.7/25.9	17.2/24.0	22.3/26.9
No. atoms			
Protein	1111	752	2979
Water	34	98	180
B-factors			
Protein	28.78	12.32	38.29
Water	32.17	22.61	43.34
R.m.s deviations			
Bond lengths [Å]	0.007	0.006	0.008
Bond angles [°]	1.027	0.871	1.032
Ramachandran plot			
Most favored [%]	97.78	96.84	98.63
Additional allowed [%]	2.22	3.16	1.37

*Values in parentheses are for the highest resolution shell.

†$R_{merge} = \sum_h \sum_l |I(h)_l - \langle I(h)\rangle| / \sum_h \sum_l I(h)_l$, where $I(h)_l$ is the lth observation of the reflection h and $\langle I(h)\rangle$ is the weighted average intensity for all observations l of reflection h.

‡$R_{work} = \sum_h ||F_{obs}(h)| - |F_{cal}(h)|| / \sum_h |F_{obs}(h)|$, where $F_{obs}(h)$ and $F_{cal}(h)$ are the observed and calculated structure factors for reflection h, respectively.

§R_{free} was calculated as R_{work} using the 10% of reflections for ENTH and Habc, and 5% of reflections for the complex, which were selected randomly and omitted from refinement.